CHINESE JOURNAL OF PHYSICS VOL. 52, NO. 1-I February 2014

The Lift Force on a Spherical Particle in Rectangular Pipe Flow

Houhui Yi*

Institute of Theoretical Physics, Department of Opto-Electronic Engineering, Binzhou University, Binzhou 256603, China

(Received February 22, 2012; Revised March 14, 2013)

The inertial migration of a neutrally buoyant particle in a rectangular pipe is investigated by lattice Boltzmann simulations. The hydrodynamic force on the particle is evaluated by the method of stress-integration and the sphere surface mesh generation technique. The lift forces at different positions, which are a component of the hydrodynamic forces and are vertical to the x-axis at steady state in constrained simulations, are calculated numerically. The particle equilibrium position is deduced at the point of zero lift force, and a stable or unstable equilibrium position is obtained by analyzing the lift force near the point of zero lift force. The dependence of the particle size and flow Reynolds number on the particle equilibrium positions is investigated. The lift force can be used to predict the moving behaviour of the particle confined by more complicated walls.

DOI: 10.6122/CJP.52.174 PACS numbers: 47.11.-j, 47.10.-g, 47.57.ef

I. INTRODUCTION

The study of the migration and equilibrium position of solid particles in shear flows is of great interest due to its broad engineering applications [1, 2]. Segré and Silberberg found that the particles in tube Poiseuille flows migrate away both from the wall and the centerline and reach a certain lateral equilibrium position of approximately $0.6r_0$, where r_0 is the radius of the cylinder [3, 4]. This remarkable phenomenon, called the Segré-Silberberg effect, has been verified by many experimental works [5–7]. It is also found that the particle's equilibrium position is closer to the wall for larger flow rates and closer to the centre for larger particles [5].

In order to explain the Segré-Silberberg effect, the lift force, which causes the particle to migrate transversely, has been studied extensively. Rubinow and Keller studied the transverse force on a spinning sphere moving in a viscous fluid [8]. Saffman obtained the lift on a small sphere in slow shear flow in an unbounded domain [9]. Ho and Leal [10] and Vasseur and Cox [11] investigated the lateral migration of a spherical particle in both a Couette flow and a plane Poiseuille flow bounded by two infinite plane walls. Schonberg and Hinch analyzed a small sphere in plane Poiseuille flow for the channel Reynolds number of order unity [12], and McLaughlin studied the lift on a small sphere in wall-bounded linear shear flows for small particle Reynolds numbers [13].

Numerical simulations of the motion of a two-dimensional circular particle in

*Electronic address: houhuily@163.com

Poiseuille flows have been performed by Feng *et al.* [14], Patankar *et al.* [15], and Joseph *et al.* [16] by using an arbitrary Lagrangian-Eulerian (ALE) technique. Zhu *et al.* extended the scheme to perform three-dimensional simulations of the migration and interaction of spheres in various flows [17]. This three dimensional ALE scheme was used by Yang *et al.* to study the migration of a sphere in tube flow [18].

The lattice Boltzmann method (LBM) [19–21] has been proven to be an alternative numerical method for simulating fluid flows in various physical and engineering systems, especially in the area of complex fluids. The calculation of hydrodynamic force acting on the particle is very important in the study of particle suspensions in fluid flows. In 2000, Inamuro *et al.* [22] proposed a method for calculating the hydrodynamic force exerted on the solid-liquid surface. Li *et al.* [23] used this equation, together with a boundary condition proposed by Filippova *et al.* [24], to evaluate the hydrodynamic force on the cylinders in a solid-fluid flow system in two dimensions. Recently, we have proposed a force evaluation method based on the stress-integration method and the sphere surface mesh generation technique in a three-dimensional lattice Boltzmann model [25]. The accuracy of the scheme was demonstrated by comparing the results with those of experiments [3, 5].

The lift force is generated by the gradient of the shear rate and the interactions of the flow field with the container walls. The lift force on a neutrally buoyant particle in tube Poiseuille flow was studied by Yang *et al.* [18]. The particle moving behaviour in a cylinder is predicted by investigating the lift force. In order to investigate the geometric effect of wall confinement on the particle motion, Chun *et al.* studied the inertial migration of neutrally buoyant particles and equilibrium positions in a square duct [26]. In this paper, we focus on the study of lift forces on a particle confined by a rectangular pipe. The lift forces at some special positions are computed and the stable or unstable equilibrium positions are obtained by analyzing the lift forces near the point of zero lift force. The dependence of the particle size and flow Reynolds number on the equilibrium positions is investigated numerically. The paper is organized as follows. In Sec. II and III, we briefly describe the lattice Boltzmann model and the method of force evaluation scheme on particles, respectively. In Sec. IV, we present our simulation results and discussions. And finally, our conclusion is presented in Sec. V.

II. THE LATTICE BOLTZMANN MODEL

The LBM is constructed by discretizing the continuous Boltzmann equation in space and time. In this study, we work on a three-dimensional cubic lattice (Q15D3) with 15 discrete velocities. Let $f_i(\mathbf{x}, t)$ be a non-negative real number describing the distribution function of the fluid density at site $\mathbf{x}$ at time t moving in the direction $\mathbf{e}_i$. Here $\mathbf{e}_0 = (0, 0, 0)$, $\mathbf{e}_i = (\pm 1, 0, 0)$, $(0, \pm 1, 0)$, $(0, 0, \pm 1)$, for $i = 1, 2, \cdots, 6$, and $\mathbf{e}_i = (\pm 1, \pm 1, \pm 1)$, for $i = 7, 8, \cdots, 14$ are the 15 possible velocity vectors. The distribution functions evolve according to a Boltzmann equation that is discrete in both space and time [19, 21],

$$f_i(\mathbf{x} + \mathbf{e}_i, t + 1) - f_i(\mathbf{x}, t) = -\frac{1}{\tau}(f_i - f_i^{eq}). \tag{1}$$

The density ρ and macroscopic velocity $\mathbf{u}$ are defined by

$$\rho = \sum_i f_i, \quad \rho\mathbf{u} = \sum_i f_i \mathbf{e}_i, \tag{2}$$

and the equilibrium distribution functions f_i^{eq} are usually supposed to be dependent only on the local density ρ and flow velocity $\mathbf{u}$. A suitable choice reads [19, 21]

$$f_i^{eq} = \rho\alpha_i \left[1 + 3\mathbf{e}_i \cdot \mathbf{u} + \frac{9}{2}(\mathbf{e}_i \cdot \mathbf{u})^2 - \frac{3}{2}u^2\right], \tag{3}$$

with

$$\alpha_i = \begin{cases} 2/9, & i = 0, \\ 1/9, & i = 1, 2, \cdots, 6, \\ 1/72, & i = 7, 8, \cdots, 14. \end{cases} \tag{4}$$

p and ν are the pressure and kinematic viscosity, defined by the equations $p = c_s^2\rho$ with $c_s^2 = 1/3$ and $\nu = (2\tau - 1)/6$, respectively.

The macroscopic equations can be derived from the lattice Boltzmann model via a Chapman-Enskog procedure [19, 21]. They are the continuity equation,

$$\partial_t \rho + \partial_\alpha(\rho u_\alpha) = 0, \tag{5}$$

and the Navier-Stokes equations,

$$\partial_t(\rho u_\alpha) + \partial_\beta(\rho u_\alpha u_\beta) = \partial_\alpha p + \nu\partial_\beta[\rho(\partial_\alpha u_\beta + \partial_\beta u_\alpha)]. \tag{6}$$

III. METHOD FOR THE FORCE EVALUATION SCHEME ON A PARTICLE

The hydrodynamic force and torque exerted on the particle are calculated by the equations [22]

$$\begin{aligned} \mathbf{F} &= \int_S \{\sigma \cdot \mathbf{n} - \rho\mathbf{u}[(\mathbf{u} - \mathbf{V}) \cdot \mathbf{n}]\}\mathrm{d}S, \\ \mathbf{T} &= \int_S \mathbf{r} \times \{\sigma \cdot \mathbf{n} - \rho\mathbf{u}[(\mathbf{u} - \mathbf{V}) \cdot \mathbf{n}]\}\mathrm{d}S, \end{aligned} \tag{7}$$

respectively. In Equation (7), S is the surface of the particle, $\mathbf{n}$ is the unit outward normal vector on S, $\mathbf{r}$ is a vector from the center of the particle to the point on S, and $\mathbf{V}$ is the velocity of the mass center of the solid particle. The stress tensor can be calculated as follows:

$$\sigma_{ij} = -\frac{1}{6\tau}\rho\delta_{ij} - \left(1 - \frac{1}{2\tau}\right)\sum (e_{\alpha i} - u_i)(e_{\alpha j} - u_j) f_\alpha, \tag{8}$$

where f_α is assumed as that of the nearest fluid node in calculating σ_{ij} on $\mathrm{d}S$, δ_{ij} is the Kronecker delta function, and $i, j = x, y, z$.

A mesh generation method on the sphere surface is used to calculate the hydrodynamic force and torque on the particle. Initially, an inscribed regular octahedron is made for the sphere. Each edge of the octahedron is projected onto the sphere surface to divide the full surface of the sphere into eight equivalent sections. Then we put m nodes on each arc of each section with an equi-distance between nearest-neighboring nodes. The inscribed octahedron vertices are named as nodes. The parallels, connected by the nodes, of each arc divide the sphere surface into $n = 8[1 + 3 + \cdots + (2m + 1)]$ subsections. The triangles, having the common nodes with the subsections, are used to replace the sphere surface. The integral in Equation (7) is approximated by the numerical quadrature of $n = 3200$ triangles in our simulations [25].

The translation of the mass center of each particle is updated at each Newtonian dynamics time step by using a so-called half-step 'leap-frog' scheme [27]. The scheme is written as

$$\mathbf{V}\left(t + \frac{1}{2}\delta t\right) = \mathbf{V}\left(t - \frac{1}{2}\delta t\right) + \delta t\mathbf{F}(t)/M, \tag{9}$$

$$\mathbf{R}(t + \delta t) = \mathbf{R}(t) + \delta t\mathbf{V}\left(t - \frac{1}{2}\right) + \delta t^2\mathbf{F}(t)/M, \tag{10}$$

where $\mathbf{V}$ and $\mathbf{R}$ denote the velocity and the position of the mass center of the solid particle, and M is the mass of the solid particle. The rotations of the particles are updated in a similar way.

IV. RESULTS AND DISCUSSIONS

Fig. 1 shows the schematic diagram of a sphere in a Poiseuille flow confined by a rectangular pipe. In this study, we perform constrained simulations. In the simulations, the particle is only allowed to move along a line parallel to the x-axis and rotate freely; its y-directional and z-directional position is fixed. The lift forces, which are the components of the hydrodynamic force on the particle and are perpendicular to the x-axis, at different positions are calculated after the simulation of the system has reached a steady state. The lift forces are related to the particle positions, and the points where the lift forces are zero are the particle equilibrium positions. The particle stable or unstable equilibrium position is also obtained by analyzing the direction of the lift force near the point of zero lift force. The investigation of the lift force can be used to predict the particle motions and equilibrium properties.

A 2D projection of the schematic diagram is shown in Figure 2. The particle is projected onto the velocity gradient plane, perpendicular to the direction of the flow. The width of the pipe are denoted by H and D, respectively. The diameter of the sphere is denoted by d. The length L of the pipe is 120 in each simulation. There exists 4 symmetry

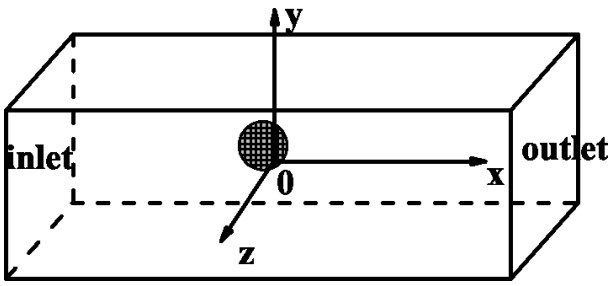

FIG. 1: Schematic diagram of a sphere in rectangular Poiseuille flow.

axes for the square pipe ($H = D$) and 2 symmetry axes for the rectangular pipe ($H \neq D$), which reflects the broken symmetry of the pipe compared with a cylinder. The Reynolds number of the flow is defined as $Re = (H + D)u/2\nu$, where u is the average velocity of the flow without particles in the pipe and ν is the kinematic viscosity of the fluid. In the study, the pressure drop between the inlet and outlet is set to be 5.88×10^{-3} (i.e., the density difference between the inlet and outlet is 1.76×10^{-2}) and consequently the pressure gradient dp/dx is -4.90×10^{-5}, which is used to produce Poiseuille flow. $\tau = 0.8$ and the fluid is assumed to have Newtonian incompressible flow with a density of 1 in a lattice unit.

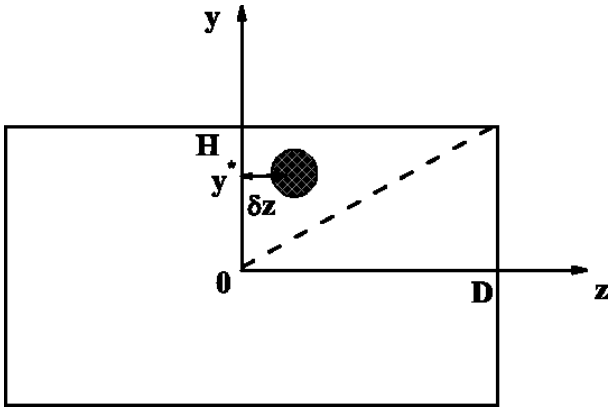

FIG. 2: A 2D projection of the schematic diagram of a sphere in a rectangular Poiseuille flow. The particle is projected onto the velocity gradient plane, perpendicular to the direction of the flow.

Initially the distribution functions at all the fluid nodes are set to be equilibrium distribution functions with zero velocity, except for those at the inlet and outlet. The boundary condition proposed in References [24, 28] is applied for the fixed curved boundaries. The boundary condition for the moving particle is treated by the method depicted in Ref. [23]. Periodical boundary conditions with a pressure difference are implemented at the inlet and outlet [29]. At the beginning the particle is situated at rest and we let the fluid flow develop and approach a steady state driven by pressure drop. At t= 10 000 time steps, the particle is released and will migrate in the tube flow. In the simulation, we let the

computational region and the particle move together, so the particle mass centre is always $L/2$ away from the inlet and outlet of the channel.

IV-1. Lift force of a particle in a square pipe

Fig. 3 displays the z directional lift forces F_z acting on the particle in pressure driven flow in a square pipe. Both D and H of the pipe are set to be 40 in lattice units. The squares in Figure 3 show the z directional lift forces as a function of the position of the center of the particle for $y = 0$. The y directional lift force F_y exerted on the particle is zero. The z component lift force $F_z > 0$ implies that the particle set at this location will migrate outwards while $F_z < 0$ means that the particle located at this site will move inwards, and $F_z = 0$ means that the particle located at this position will not move laterally, and thus this zero lift force point is a equilibrium position. The lift force first increases and then decreases with increasing z when $0 < z/D < 0.55$. The lift force increases with increasing z when $z/D > 0.55$ but the direction of the lift force is towards the pipe center. The particle finds its equilibrium position on the z axis with the value of $z/D = 0.55$, where the lift force is zero. Due to the symmetry of the system, the other three equilibrium positions can be obtained similarly. The pipe center is an unstable equilibrium position, even though the lift force is zero, because the direction of the lift force near the center of the pipe is outwards and a little disturbance will push the particle out-of-center. To illustrate that an equilibrium position is stable or unstable at the point of zero lift force, the forces near the point of zero lift force are studied, as shown in Figure 4. $F_y < 0$ if $y > 0$ while $F_y > 0$ if $y < 0$, and larger absolute value y leads to larger $|F_y|$. F_y almost has the same behaviour as that of a restoring force, which results in the particle finding its final position at $z^* = 0.55D$ on the z axis. The slope of the curve in Figure 3 at the point of zero lift force can be also used to distinguish a stable or unstable equilibrium position. If the slope is negative, this zero lift force point is a stable equilibrium position. When the slope is positive, this zero lift force point is an unstable equilibrium position.

The triangles in Figure 3 display the variance of the lift forces with respect to particle positions near a corner of the pipe. At the corner, the particle has two nearest walls, so the wall confinement effect on the particle is stronger than that of one placed at the center of an edge. The equilibrium position y^*/H (z^*/D) is 0.45, which is smaller than that of the $y = 0$ case. The normal lift force, which is vertical to the line of $y = z$, is denoted by F_n. The force F_n for different δ is also shown in Figure 5. $F_n < 0$ if $\delta > 0$ while $F_n > 0$ if $\delta < 0$, and a larger absolute value δ leads to a larger $|F_n|$. The particle stable equilibrium position at this corner is predicted by analyzing the lift force. Due to the symmetry of the system, we have obtained up to 8 equilibrium positions, similar to the results found experimentally.

Fig. 6 shows the particle equilibrium positions at the center near the upper edge. The pressure drop between the inlet and outlet is set to be 1.18×10^{-2} and 1.76×10^{-2}, respectively, for $Re = 24.2$ and 36.3. The particle moves closer to the upper wall with increasing flow Reynolds number. The equilibrium position is shifted farther from the wall with increasing particle size. The same feature has also been obtained when the sphere stabilizes at the other seven positions. The simulation results are in agreement with theory

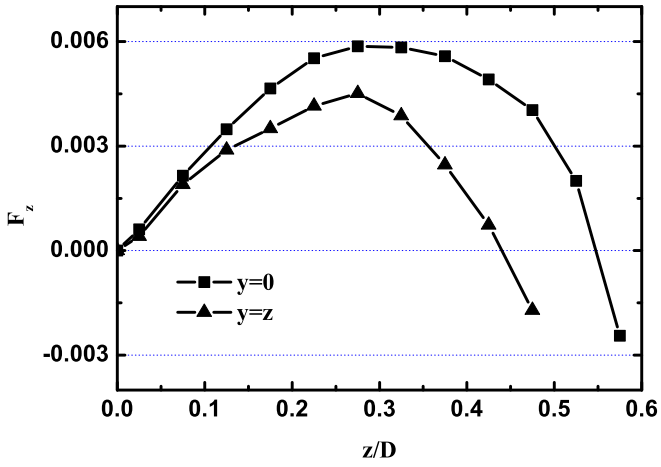

FIG. 3: The particle z component lift forces F_z in the steady state for different particle positions z at $d/D = 0.3$ and $Re = 12.1$. The squares and triangles denote that the center of the sphere is constrained at $y = 0$ and $y = z$, respectively.

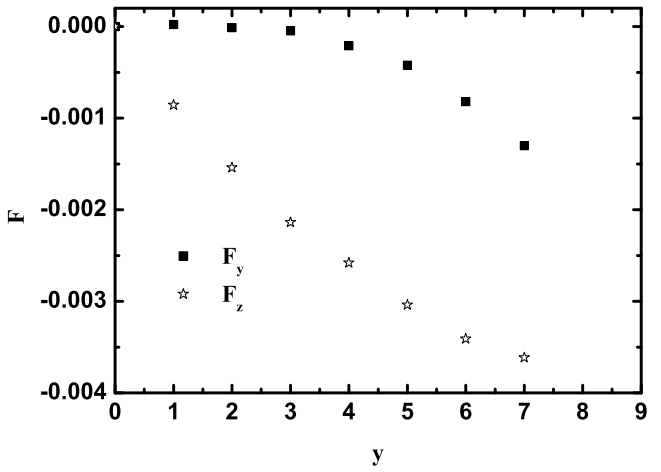

FIG. 4: The particle lift forces F_y and F_z in steady state as a function of particle positions y for $z/D = 0.55$.

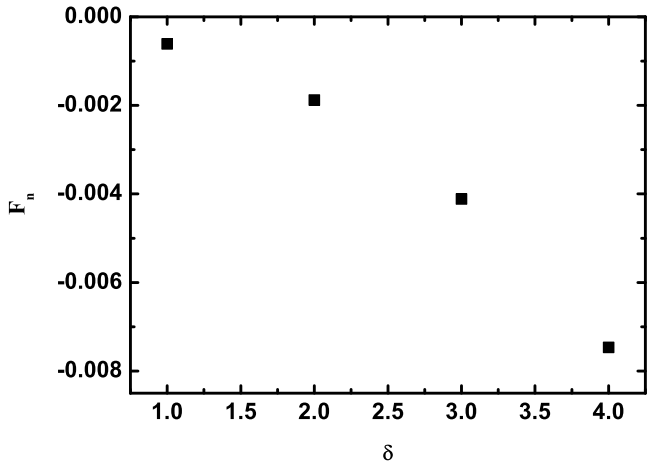

FIG. 5: The particle lift forces F_n in steady state for different δ. δ is defined as $\sqrt{2}(y - y^*)$.

and experiment [3, 26].

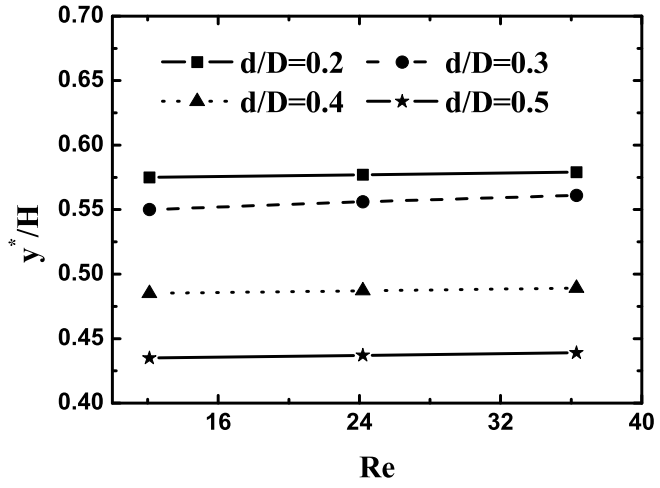

FIG. 6: Particle equilibrium positions in the square pipe.

IV-2. Lift force of a particle in a rectangular pipe

Fig. 7 (a) and (b) display the simulation results of the y directional lift force F_y with respect to particle positions y for $z = 0$ and the z directional lift force F_z versus particle positions z for $y = 0$, separately. The lift force F_y (or F_z) first increases and then decreases to zero with increasing z, and finally increases with increasing y (or z). In the simulation, H and D are set to be 40 and 60, respectively. D is larger than H, and the confinement of the walls results in a larger shear rate along the y axis than that along the z axis. The blockage ratio d/D is smaller than d/H. The equilibrium position y^*/H at $z = 0$ is smaller than that of z^*/D at $y = 0$. The effect of the particle size on different equilibrium positions is also shown in Figure 8.

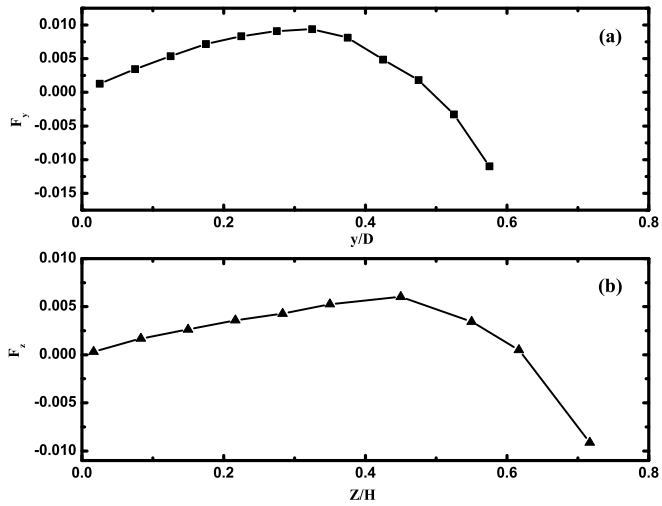

FIG. 7: The particle y (or z) component lift forces F_y (or F_z) in steady state for different particle positions y (or z) when the particle is restrained at the y (or z) axis for $d/D = 0.3$ and $Re = 20.8$.

V. CONCLUSIONS

In summary, we used a lattice Boltzmann method to examine the inertial migration of a neutrally buoyant particle in a rectangular pipe in a pressure driven flow. The hydrodynamic lift forces acting on the particle are calculated, and the particle equilibrium positions are obtained numerically. The particle equilibrium positions are determined by the interplay between the background flow field and the pipe shape of the boundary. The particle moving behaviour can be predicted by investigating the lift force. In our future work, we will focus on the study of the fluid dynamic mechanisms of deformable particles confined by complicated walls.

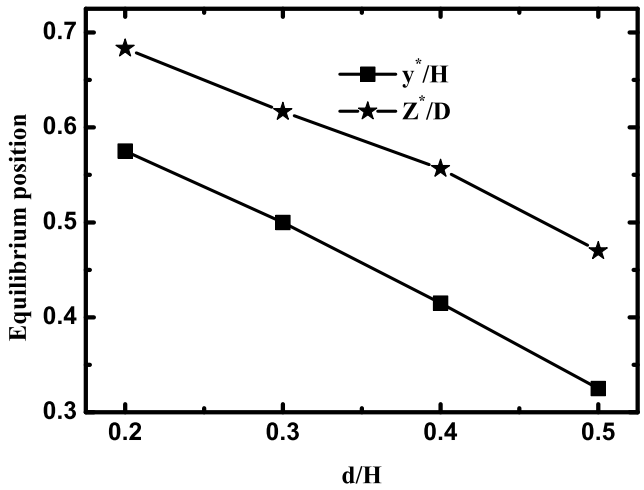

FIG. 8: Particle equilibrium position in the rectangular pipe.

Acknowledgements

We sincerely thank the referee for his suggestions and comments that helped us to make a more efficient paper. This work was supported by the Natural Science Foundation of Shandong Province under Grant Nos. ZR2011AM001 and ZR2011AL020, and the Science and Technology Development Projects of Shandong Province of China under Grant No. 2011YD18027.

References

[1] Y. C. Fung, *Biomechanics Circulation* (Springer-Verlag, Berlin, 1997).
[2] D. E. Smith, H. P. Babcock, and S. Chu, Science **283**, 1724 (1999). doi: 10.1126/science.283.5408.1724
[3] G. Segré and A. Silberberg, Nature **189**, 209 (1961).
[4] G. Segré and A. Silberberg, J. Fluid Mech. **14**, 115 (1962).
[5] A. Karnis, H. L. Goldsmith, and S. G. Mason, Can. J. Chem. Eng. **44**, 181 (1966). doi: 10.1002/cjce.5450440401
[6] E. Bartram, H. L. Goldsmith, and S. G. Mason, Rheol. Acta. **14**, 776 (1975). doi: 10.1007/BF01521406
[7] J. Feng, and D. D. Joseph, J. Fluid Mech. **324**, 199 (1996). doi: 10.1017/S0022112096007896
[8] S. I. Rubinow and J. B. Keller, J. Fluid Mech. **11**, 447 (1961). doi: 10.1017/S0022112061000640
[9] P. G. Saffman, J. Fluid Mech. **22**, 385 (1965). doi: 10.1017/S0022112065000824
[10] B. P. Ho and L. G. Leal, J. Fluid Mech. **35**, 365 (1974).

[11] P. Vasseur and R. G. Cox, J. Fluid Mech. **78**, 385 (1976). doi: 10.1017/S0022112076002498
[12] J. A. Schonberg and E. J. Hinch, J. Fluid Mech. **203**, 517 (1989). doi: 10.1017/S0022112089001564
[13] J. B. McLaughlin, J. Fluid Mech. **246**, 249 (1993). doi: 10.1017/S0022112089001564
[14] J. Feng, H. H. Hu, and D. D. Joseph, J. Fluid Mech. **277**, 271 (1994).
[15] N. A. Patankar, P. Y. Huang, T. Ko, and D. D. Joseph, J. Fluid Mech. **438**, 67 (2001). doi: 10.1017/S0022112001004104
[16] D. D. Joseph and D. Ocando, J. Fluid Mech. **454**, 263 (2002). doi: 10.1017/S0022112001007145
[17] M.-Y. Zhu, Direct numerical simulation of the solid-liquid flows of Newtonian and viscoelastic fluids (PhD thesis, University of Pennsylvania, 2000)
[18] B. H. Yang, J. Wang, D. D. Joseph, H. H. Hu, T. -W. Pan, and R. Glowinski, J. Fluid Mech. **540**, 109 (2005). doi: 10.1017/S0022112005005677
[19] Y. H. Qian, D. d'Humiéres, and P. Lallemand, Europhys. Lett. **17**, 479 (1992). doi: 10.1209/0295-5075/17/6/001
[20] S. Y. Chen and G. D. Doolen, Annu. Rev. Fluid Mech. **30**, 329 (1998). doi: 10.1146/annurev.fluid.30.1.329
[21] S. Chen, H. Chen, D. O. Martinez, and W. H. Matthaeus, Phys. Rev. Lett. **67**, 3776 (1991). doi: 10.1103/PhysRevLett.67.3776
[22] T. Inamuro, K. Maeba, and F. Ogino, Int. J. Multiphase Flow **26**, 1981 (2000). doi: 10.1016/S0301-9322(00)00007-0
[23] H. B. Li, X. Y. Lu, H. P. Fang, and Y. H. Qian, Phys. Rev. E **70**, 026701 (2004). doi: 10.1103/PhysRevE.70.026701
[24] O. Filippova and D. Hanel, Comput. Fluids. **26**, 697 (1997). doi: 10.1016/S0045-7930(97)00009-1
[25] H. H. Yi, L. J. Fan, and Y. Y. Chen, Int. J. Mod. Phys. C **20**, 831 (2009). doi: 10.1142/S0129183109014035
[26] B. Chun and A. J. C. Ladd, Phys. Fluids **18** 3, 031704, 2006. doi: 10.1063/1.2176587
[27] M. P. Allen and D. J. Tildesley, *Computer Simulation of Liquid* (Clarendon Press, Oxford 1987).
[28] R. Mei, W. Shyy, D. Yu, and L. S. Luo, J. Comp. Phys. **161**, 680 (2000). doi: 10.1006/jcph.2000.6522
[29] T. Inamuro, M. Yoshino, and F. Ogino, Int. J. Numer. Meth. Fluids **29**, 737 (1999). doi: 10.1002/(SICI)1097-0363(19990415)29:7<737::AID-FLD813>3.0.CO;2-H